

## Influence of Southern Hemisphere Winds on North Atlantic Deep Water Flow

STEFAN RAHMSTORF

*Potsdam Institute for Climate Impact Research, Potsdam, Germany*

MATTHEW H. ENGLAND

*School of Mathematics, University of New South Wales, Sydney, Australia*

(Manuscript received 12 November 1996, in final form 24 March 1997)

### ABSTRACT

A series of experiments with a hybrid model (ocean circulation model with simple atmospheric feedback model) and an ocean-only model is used to study the sensitivity of the ocean's deep overturning circulation to Southern Hemisphere winds. In particular, the "Drake Passage effect" is examined.

The results show that two factors weaken the control that the Drake Passage effect exerts over the flow of North Atlantic Deep Water (NADW). The first is that thermohaline forcing alone can generate about 75% of the NADW flow found in our model; this ability is lost if atmospheric feedback is neglected. The second is that about two-thirds of the downwelling induced by Ekman transport across Drake Passage occurs in the Southern Hemisphere just north of Drake Passage; only one-third occurs in the North Atlantic and enhances NADW flow. For these two reasons, the influence of Southern Ocean winds on NADW flow is only moderate and not as strong as previously suggested. However, the authors find that the formation rate of Antarctic Bottom Water depends strongly on the winds over the Southern Ocean.

### 1. Introduction

Toggweiler and Samuels (1993a, hereafter TS93) and Toggweiler and Samuels (1995, hereafter TS95) have proposed that the formation rate of North Atlantic Deep Water (NADW) is largely dictated by the winds in the Southern Hemisphere at the latitude of Drake Passage, through a climatic teleconnection which they call the "Drake Passage effect." At this latitude, strong westerly winds force a northward Ekman drift of an estimated 17 Sv (TS95). The water pushed north in this way has to return southward at depth; it must do so largely below the depth of some topographic ridges at this latitude, as above the topography no mean zonal pressure gradient, and thus no geostrophic southward flow, can be supported. Toggweiler and Samuels argue that in order to get down to the depth required ( $\sim 1500$  m), the water pushed north by the wind across the latitude of the tip of South America in any of the three oceans must sink in the North Atlantic as NADW; everywhere else the ocean is too stratified for deep downwelling to occur. They conclude that the southward NADW outflow from the Atlantic basin (we use this term here for the enclosed part of the Atlantic north of the Cape of Good Hope)

varies in direct proportion to the amount of northward Ekman drift. They go on to suggest that in high-resolution models NADW outflow must *equal* the Ekman drift (TS93), while in low-resolution models it is somewhat less due to the artificially high viscosity in these models.

A direct 1:1 relationship of NADW outflow rate and Southern Hemisphere Ekman drift would exist if (i) thermohaline forcing was unable to draw surface waters across  $30^{\circ}\text{S}$  into the Atlantic basin and generate outflow on its own, and if (ii) the water pushed north in the Ekman drift had no other way to return south than via the Atlantic basin. At least in coarse-resolution models neither of these conditions holds.

For example, England (1992) compares two model experiments with and without wind stress. Both have very similar meridional overturning patterns in the Atlantic (see Fig. 1), except that the shallow Ekman cells are absent and the intensity of the deeper flow is reduced by about 25% in the no-wind case (NADW outflow is reduced to 9 Sv from 12 Sv). This shows that thermohaline forcing on its own can generate a NADW circulation close to that observed. On the other hand, Cox (1989) shows a model experiment (his experiment 3, reproduced in TS93) that includes wind forcing but produces no NADW outflow, in spite of a NADW formation rate of over 10 Sv ( $\text{Sv} \equiv 10^6 \text{ m}^3 \text{ s}^{-1}$ ). Manabe and Stouffer (1988) among others (see review by Rahmstorf et al. 1996) found a "southern sinking state"

---

*Corresponding author address:* Dr. Stefan Rahmstorf, Potsdam Institute for Climate Impact Research, P.O. Box 60 12 03, 14412 Potsdam, Germany.  
E-mail: Rahmstorf@pik-potsdam.de

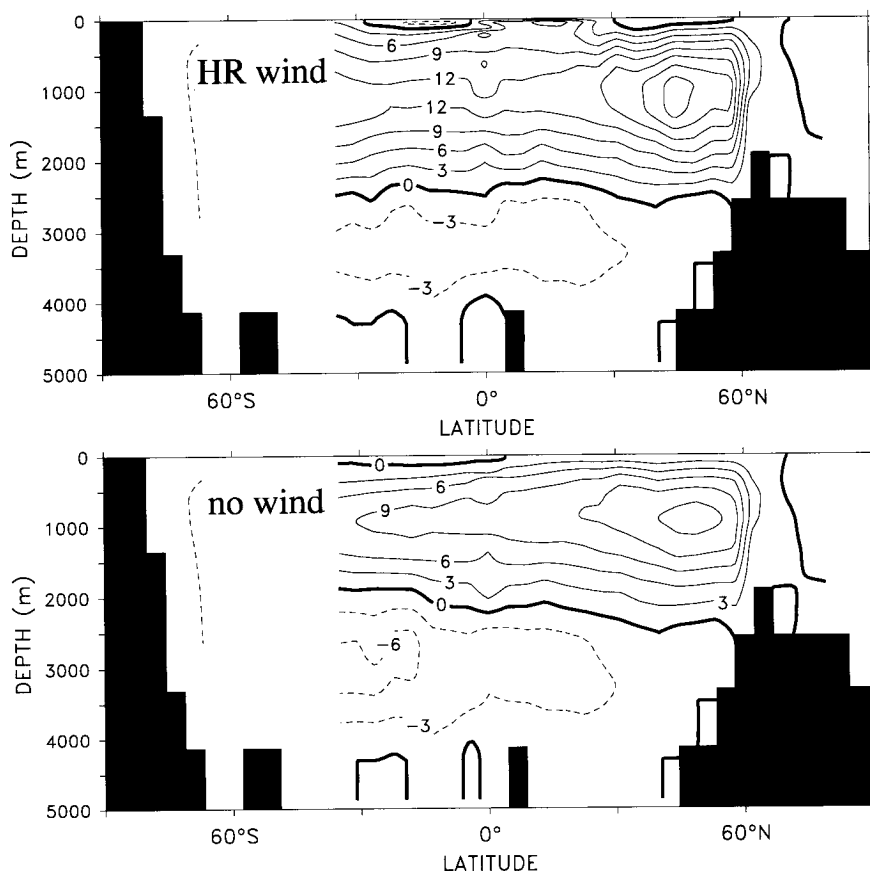


FIG. 1. Meridional transport streamfunction for the Atlantic in the global model of England (1992): (a) with wind forcing from Hellerman and Rosenstein (1983) and (b) without wind forcing.

of their coupled model with no NADW outflow. Hughes and Weaver (1994) found multiple equilibria with widely differing NADW overturning and outflow rates for the same (mixed) boundary conditions in an idealized model. Hughes (1995) lists over 30 model experiments with different wind stress and initial conditions, and shows that the outflow from the North Atlantic can be either much smaller or much larger than the northward Ekman drift (see her Fig. 2.21). While mixed boundary conditions (i.e., restoring temperature and prescribing a fixed freshwater flux) are known to induce a thermohaline feedback that is unrealistically unstable, it is clear that the wind forcing (at least in coarse models) does not put a hard constraint on the NADW outflow and that there are ways to return the water pushed north in the Ekman drift to the south even in the absence of NADW outflow from the Atlantic basin.

Toggweiler and Samuels argue that these alternative return routes for the northward drift are not used once a NADW outflow is established, and that the Ekman drift “locks on” to the NADW flow. It is equally possible, however, that only part of the Ekman drift will choose to ride with the NADW flow through the Atlantic. How large this part is will then determine how strong the influence of Southern Hemisphere winds is

on NADW production and outflow. This could well depend on the diapycnal mixing and viscosity of the model and thus on its resolution, as TS93 point out.

Ultimately, however, their arguments rest on empirical evidence from coarse-resolution model experiments. Some high-resolution experiments are available for comparison, but these are of limited use as they are run for short time periods only and often in robust-diagnostic mode (i.e., with interior restoring to observations; Semtner and Chervin 1992), so that in either case they show no dynamically consistent deep circulation. The deep water renewal by convection depends on a subtle balance between the ocean’s interior density field and surface forcing, which is established on a diffusive timescale (hence the long spinup time of several thousand years for the deep circulation). While the interior density field is still determined by the initial condition or is artificially maintained by interior restoring, this balance need not be closed and the deep circulation may have an unrealistic parameter dependence. As an example, it is well known that the strength of the deep circulation increases with increased vertical diffusivity since diapycnal diffusion is its ultimate driving force. However, 30 or 50 years after model initialization, diffusion can hardly affect the deep flow since it has had

no time yet to change the prescribed initial density field. As we are interested in the long-term dynamical balance here (and not in the effect that short-term wind bursts in the Southern Hemisphere might have), only long model runs are of use here.

The purpose of this paper is to present new model experiments investigating the sensitivity of the deep circulation to Southern Hemisphere winds. In contrast to previous experiments with restoring or mixed boundary conditions, we provide for a more realistic thermohaline feedback by using a simple atmospheric energy balance model (Rahmstorf and Willebrand 1995) in combination with fixed freshwater fluxes. Only with an approximately correct thermohaline feedback can we hope to evaluate the relative importance of thermohaline and wind forcing in setting the magnitude of NADW outflow. Furthermore, we examine the wind-dependence of the circulation across a continuous range from zero wind to twice the present-day winds over the Southern Ocean. Sharing many of the same limitations of other coarse-resolution studies, these experiments cannot provide definitive evidence about the significance of the “Drake Passage effect,” but it is hoped that they will contribute to the discussion on this intriguing subject.

## 2. Model description and experiment design

### a. A hybrid coupled model

The ocean model used in our experiments is based on the GFDL Modular Ocean Model (MOM) Version 1.1 (Pacanowski et al. 1991), and its configuration is very similar to the one used by Toggweiler and Samuels. The model is global with a resolution of  $4.5^\circ$  latitude and  $3.75^\circ$  longitude and 12 levels in the vertical; the topography of this model is shown in Rahmstorf (1995b). The model was initially spun up from rest by applying wind stress from Hellerman and Rosenstein (1983) and restoring the surface level to annual mean temperature and salinity data from Levitus (1982) (averaged over the top 50 m and interpolated to the model grid). Very low salinity values from inside the Baltic as well as the fjords of Tierra del Fuego, which affected some grid points, were rejected and replaced by typical ocean values from the region (Rahmstorf 1996a). The horizontal and vertical viscosities were  $2.5 \times 10^5$  and  $5 \times 10^{-3} \text{ m}^2 \text{ s}^{-1}$  respectively. Mixing was parameterized by depth-dependent diffusivities, varying for horizontal mixing from  $1.0 \times 10^3 \text{ m}^2 \text{ s}^{-1}$  at the surface to  $0.5 \times 10^3 \text{ m}^2 \text{ s}^{-1}$  in the deepest level, and for vertical mixing from  $0.3 \times 10^{-4}$  to  $1.3 \times 10^{-4} \text{ m}^2 \text{ s}^{-1}$ . All static instability was removed at each time step by a fast and complete convection scheme (Rahmstorf 1993). Split time stepping (Bryan 1984) was used throughout the experiments, with a tracer time step of one day and a momentum time step of one hour.

The model configuration of TS93 and TS95 differs from ours in using a smaller vertical viscosity ( $2 \times 10^{-3}$

$\text{m}^2 \text{ s}^{-1}$ ) and a slightly smaller vertical diffusivity at depth ( $1.0 \times 10^{-4} \text{ m}^2 \text{ s}^{-1}$ ). Further differences are in the convection scheme used and in the topography. In particular, the Drake Passage is deeper than ours in TS93, and they have a closed Indonesian Passage (we have a throughflow of 16 Sv from the Pacific to the Indian Ocean). The surface forcing also differs as discussed below.

The fluxes of heat and freshwater diagnosed from the equilibrated spinup of the ocean model were used in creating a simple atmospheric feedback model. The freshwater fluxes at the ocean surface are simply stored and prescribed as time-independent fields in the experiments that follow; this is based on the assumption that any feedback of ocean circulation changes on the atmospheric hydrological cycle is weak (Hughes and Weaver 1996). The heat flux is computed from the condition

$$Q = \gamma(T^* - T_o) - \mu \nabla^2(T^* - T_o) \quad (1)$$

(Rahmstorf and Willebrand 1995), where  $Q$  is the heat flux at the ocean surface,  $T_o$  the ocean surface temperature,  $\gamma$  a radiative relaxation constant ( $3 \text{ W m}^{-2} \text{ K}^{-1}$ ),  $\mu$  a constant related to atmospheric heat diffusion ( $2 \times 10^{13} \text{ W K}^{-1}$ ), and  $T^*$  defines a climate without oceanic heat transport, around which Eq. (1) is linearized. The atmospheric temperature is a diagnostic variable in this model; it is already eliminated from Eq. (1) by using an atmospheric heat budget equation. The field of  $T^*$  is calculated by inverting Eq. (1) with given heat fluxes from the spinup, so that Eq. (1) essentially represents a flux-adjusted, diffusive atmosphere [see Rahmstorf (1995b) for a more detailed discussion].

Though extremely simple, this model is a significant improvement on using restoring boundary conditions, which would assume fixed atmospheric temperature and are incapable of giving even approximately the correct sea surface temperature (SST) response to changes in oceanic heat transport. To study changes in the thermohaline circulation, it is crucial to account for this SST response, as it has an important feedback effect on density and the circulation (see Fig. 11 and related discussion below). Equation (1) is probably the simplest possible way of allowing for this feedback in an approximate way.

Using a “hybrid” model like this, with its very simple atmosphere, has the advantage that it takes only a few days on a single processor of a Cray C90 computer to integrate for several thousand years—something that is all but impossible to do with a full coupled model. If one is interested in the ocean’s deep circulation and its equilibria, such long integration times are required since this is the timescale over which the thermohaline circulation evolves. In particular, the hybrid model allows sensitivity studies by varying model parameters using the quasi-equilibrium method described in the next section.

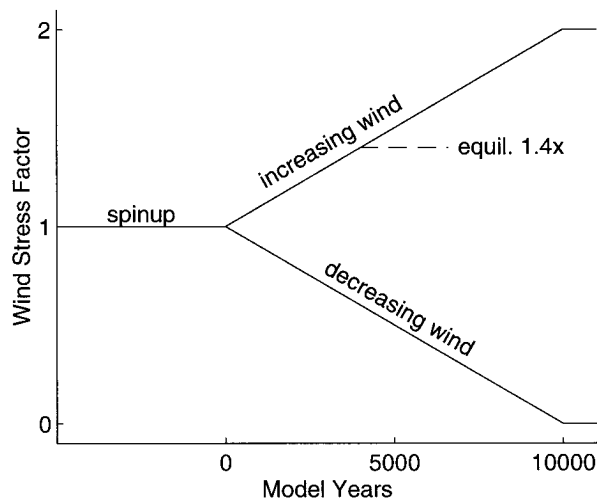


FIG. 2. Schematic of the quasi-equilibrium experiments discussed in this paper. Starting from a spinup experiment forced by constant (annual mean) wind stress (Hellerman and Rosenstein 1983), the zonal wind stress over the Southern Ocean was increased to twice its present value or decreased to zero during 10 000 model years.

*b. The quasi-equilibrium method for sensitivity studies*

The experimental philosophy followed here is the same as the one applied by Rahmstorf (1995a): the model sensitivity to a parameter is investigated by gradually changing this parameter over time, so slowly that the model can follow the change while always remaining close to equilibrium. This is similar to the classic thermodynamic quasi-equilibrium experiments described in physics textbooks. In our case, the parameter that is varied is the zonal component of the wind stress south of 30°S, which is multiplied by a factor just like in TS93 and TS95. Starting from a steady model equilibrium with present-day forcing (the wind factor being 1), the

wind factor is gradually increased to 2 in one experiment and decreased to 0 in another during the course of 10 000 model years (see Fig. 2). These same experiments were performed both with the simple atmospheric response model described in the previous section and with restoring boundary conditions (the latter only for comparison purposes).

In these experiments it is necessary to verify how close to equilibrium the model remains; this depends on the rate of change in the model and its relation to the equilibration timescale as discussed in Rahmstorf (1995a). In the case of freshwater forcing as the control parameter, the response is complicated by the nonlinear dynamics of the system and the existence of bifurcation points, near which the model response becomes very sluggish and its state deviates significantly from equilibrium. Fortunately, the wind forcing response discussed in this paper appears to be simpler. Figure 3 shows the initial response of the NADW overturning and outflow to a linear increase of the wind stress over the Southern Ocean, at a rate corresponding to a doubling of the wind stress during 10 000 model years. As expected, the circulation does not respond instantaneously to the rising wind stress but with a certain delay. We may assume that near equilibrium the NADW formation and outflow approach their equilibrium values following a simple linear feedback law,

$$\frac{dm}{dt} = \frac{(m_{eq} - m)}{\tau} \tag{2}$$

Here  $m$  denotes mass transport of either the outflow or the overturning cell, and  $m_{eq}$  is its equilibrium value; we assume that the latter increases linearly with the wind stress, at a rate equal to the slope  $s$  (in Sv/yr) of the model response in Fig. 3 after the initial adjustment is over and the flow increases linearly with time (e.g., between years 600 and 1000). Then we can determine

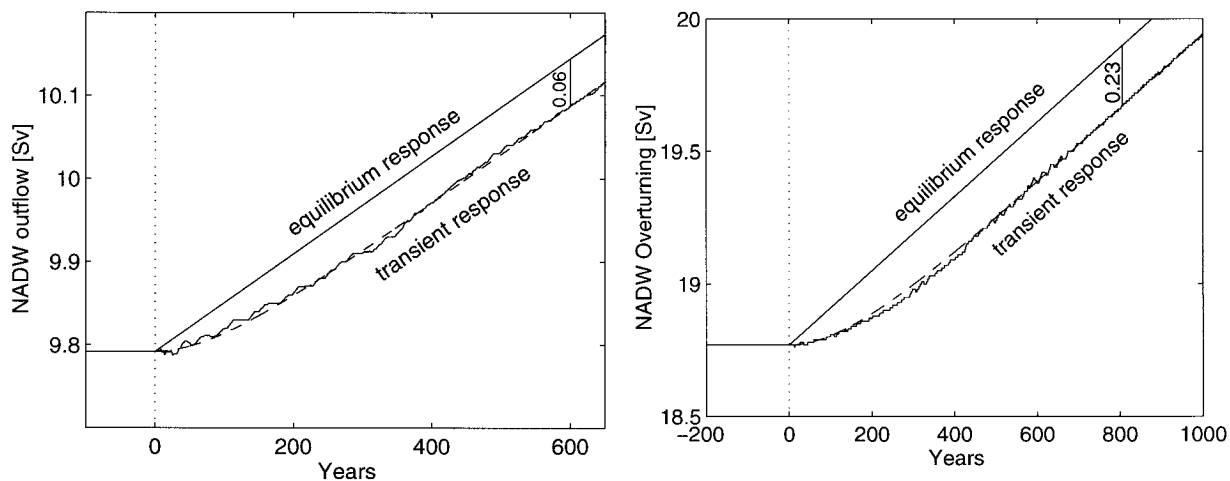


FIG. 3. Response to the switch from constant wind stress to linearly increasing wind stress. The upper solid line is the theoretical equilibrium response, the lower solid line the actual response of the ocean model, and the dashed line the response of a linear response model [Eq. (2)]. (a: left) NADW outflow for the hybrid model and (b: right) Atlantic overturning for restoring boundary conditions.

TABLE 1. Fitted parameter values for the linear response model (see text and Fig. 3).

	$s$ (Sv/kyr)	$\Delta m$ (Sv)	$\tau$ (yr)
Simple atmosphere			
Overturning	0.6	0.13	220
Outflow	0.6	0.06	100
Restoring conditions			
Overturning	1.4	0.23	165
Outflow	0.9	0.10	110

the equilibration timescale  $\tau$  from the lag  $\Delta m = m_{\text{eq}} - m$  (marked on Fig. 3), as  $\tau = \Delta m/s$ . Table 1 shows  $s$ ,  $\Delta m$ , and  $\tau$  for both outflow and overturning for restoring and simple atmosphere experiments. The outflow responds faster to Southern Ocean wind changes than the overturning. McDermott (1996) has reproduced the Drake Passage effect in an idealized model with two basins and analyzed the transient response to step-function wind changes. He found that the adjustment occurs through baroclinic waves as in the spinup problem of Kawase (1987); the initial response to wind changes was felt within years, while equilibration took centuries, consistent with our results.

Of course it is not certain that the response can be modeled with a single delay timescale as in Eq. (2); perhaps some further adjustment of the flow could occur on a longer timescale. To check this, the linear increase of wind stress was halted at 1.4 times the present-day value in one experiment, and the integration continued with constant wind stress for 2600 years. Figure 4 shows the NADW overturning of this experiment (for the simple atmosphere model). Equation (2) predicts a lag  $\Delta m$  of 0.13 Sv for this case (see Table 1), and indeed the equilibrium value found after 2600 years is 0.13 Sv higher than the transient value in our quasi-equilibrium experiment.

These results suggest that with the quasi-equilibrium method we indeed stay close to the equilibrium response that we want to analyze, though obviously this can in practice be tested only for a few points along the curve and may not be true near some points where the circulation undergoes a strongly nonlinear transition, such as a reorganization of its convection pattern. In such a case, the transient model state could be on one side of the transition point, while the true equilibrium state may be on the other. However, the Atlantic overturning and outflow vary smoothly in our experiments, and the NADW outflow in the simple atmosphere experiment appears to be within about 0.06 Sv of the equilibrium value. If an accuracy of, say, 0.3 Sv had been deemed satisfactory, then the wind stress could have been increased five times faster in the experiments, reducing the integration time for a wind stress doubling from 10000 years to only 2000 years. Depending on the required accuracy and the response time of the experiment, the quasi-equilibrium method need not be computationally expensive. An experiment with a gradual

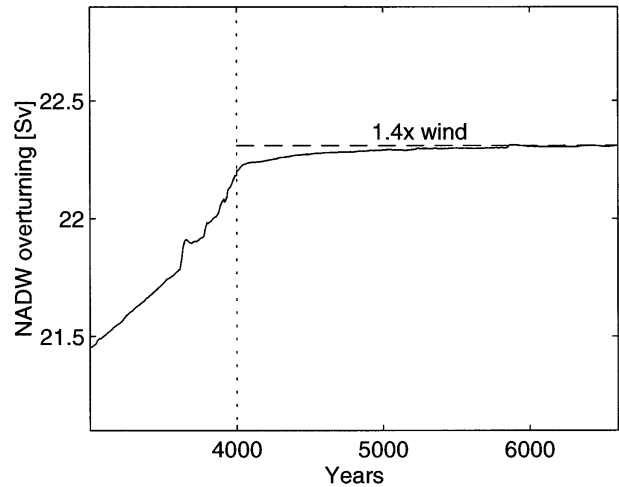


FIG. 4. Atlantic overturning in the hybrid model for an experiment where the Southern Ocean wind stress was increased to 1.4 $\times$  its present value and then kept constant. The dashed line shows the expected equilibrium value from the linear response model [Eq. (2)].

doubling of wind stress over 2000 years yields far more information than the equilibration of a fixed value of, say, 1.5 times the present-day wind stress during the same integration time.

### 3. Results

#### a. Response of the hybrid model to changes in Southern Ocean winds

At first, a preliminary experiment was performed in which the zonal wind stress over the Southern Ocean was simply switched off. A time series of the model response to this drastic forcing change is shown in Fig. 5. The North Atlantic overturning is hardly affected; it

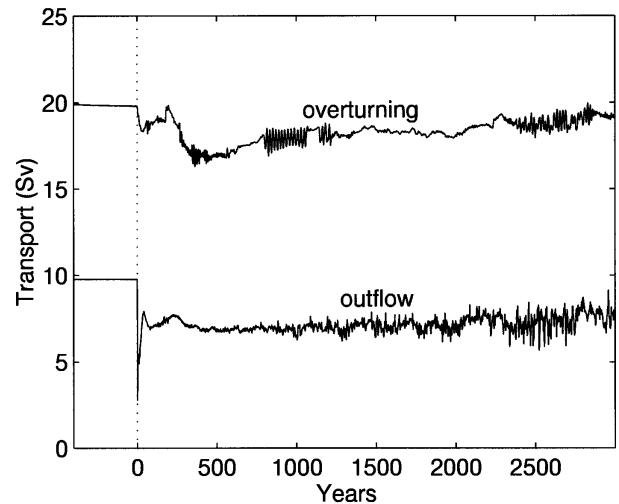


FIG. 5. Atlantic overturning and outflow in the hybrid model for an experiment where the zonal wind stress in the Southern Ocean was switched to zero at time  $t = 0$ .

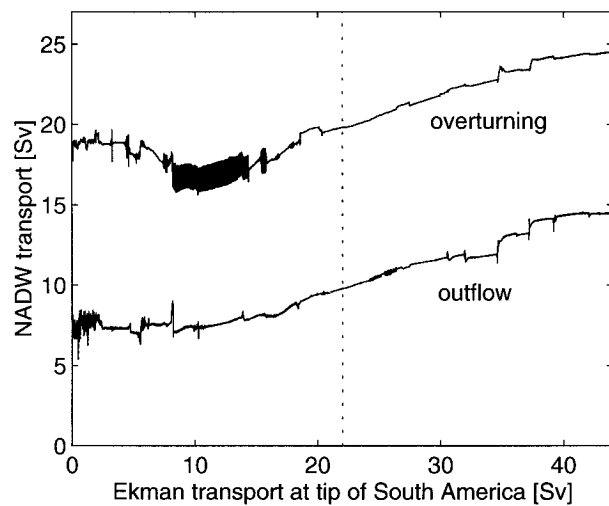


FIG. 6. Atlantic overturning and outflow in the hybrid model for the quasi-equilibrium experiments outlined in Fig. 2, plotted as function of the wind-induced Ekman transport across the latitude of the tip of South America ( $53^{\circ}\text{S}$  in our model).

drops slightly and undergoes some minor oscillations during the 3000 years of the experiment. The outflow of NADW at  $30^{\circ}\text{S}$ , in contrast, collapses almost instantaneously down to 2.5 Sv but then recovers to 7.5 Sv, indicating an initial barotropic response and subsequent baroclinic compensation. This preliminary experiment already suggests that our hybrid model may not be as sensitive to changes in Southern Ocean winds as the model of Toggweiler and Samuels forced by restoring boundary conditions.

To study the sensitivity in more detail, quasi-equilibrium experiments, as summarized in Fig. 2 and discussed in section 2b, were performed. Figure 6 shows the North Atlantic overturning and NADW outflow of the hybrid model plotted as function of the Ekman transport at the tip of South America (or more precisely, at the northernmost velocity grid point inside Drake Passage at  $53.3^{\circ}\text{S}$ ). The curves shown are, in fact, time series traced at a resolution of one year and starting in the middle of the figure (on the dotted line) at an Ekman transport of 22 Sv, reaching 0 and 44 Sv respectively after 10 000 years. The thick black traces are regions where the circulation oscillates at a period close to 20 years; this seems to be a preferred period for thermohaline oscillations in the Atlantic found in numerous model studies. "Spikes" and "jumps" in the curves occur probably where certain convection points are switched on or off; this was not investigated in detail here, but was found to be the case for similar transitions in previous studies (Rahmstorf 1995a). We did not find the strong centennial oscillations experienced by TS93 under mixed boundary conditions; these appear to be an artifact of this unrealistically unstable type of thermohaline forcing (Mikolajewicz and Maier-Reimer 1994).

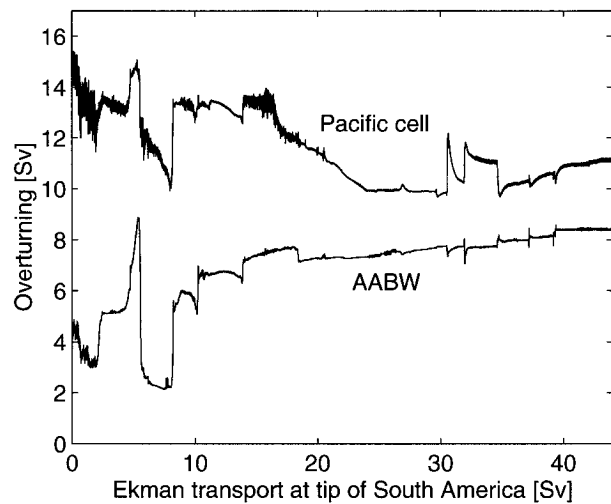


FIG. 7. As in Fig. 6 but for the overturning in the Pacific and for the Antarctic Bottom Water cell in the Atlantic.

Figure 7 shows the corresponding curves for the deep water inflow into the Indian and Pacific Oceans (combined) and the Antarctic Bottom Water (AABW) flow in the Atlantic. These circulations show a stronger and less smooth response to wind changes over the Southern Ocean. The greater sensitivity is plausible, given that the Southern Ocean is the source region for these flows. The apparent increase in overturning in the Pacific for weaker winds is misleading, however, as the structure of the overturning cell changes completely as the inflow of bottom water decreases; this will be discussed in section 3d. Below an Ekman transport of about 8 Sv large sudden transitions occur; in this parameter range we cannot assume that the curves still represent a quasi-equilibrium state. Continued integration with zero Ekman transport indeed shows that in this case the flow rate of AABW is unstable, oscillating near a baseline of 5 Sv most of the time but surging to over 10 Sv about every 1000 years.

#### b. Comparison with restoring boundary conditions

To provide a comparison with earlier model studies we repeated the same experiment with restoring boundary conditions, using a damping timescale of 50 days for both salinity and temperature (the model's upper layer is 50 m thick). The results are shown in Fig. 8. Even under restoring boundary conditions, marked interdecadal oscillations occur in the outflow. Both overturning and outflow in the Atlantic are much more sensitive to the wind changes than in the hybrid model.

Figure 9 compares the NADW outflow (smoothed and with the oscillations filtered out) of our restoring boundary condition experiment with the results of Toggweiler and Samuels. Due to the model differences, our initial state corresponding to present-day winds has a slightly weaker NADW outflow than the  $1\times$  experiment of

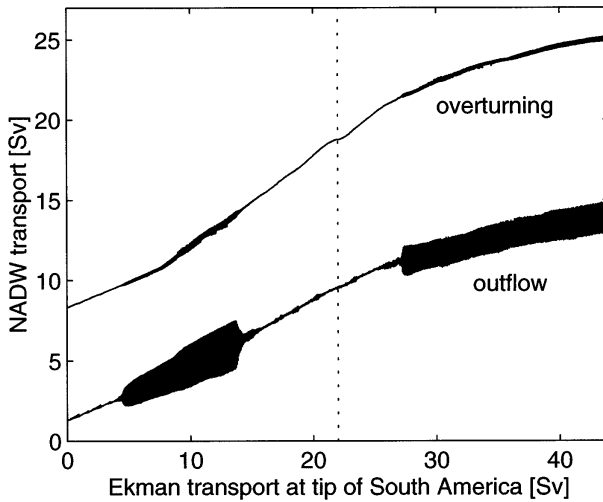


FIG. 8. As in Fig. 6 but for the model with restoring boundary conditions.

TS93. The reason is most likely their use of a 30-day restoring timescale on temperature; with that restoring timescale our model also produces a NADW outflow of 11 Sv. The sensitivity of our model to Southern Ocean winds, however, is essentially the same as in Toggweiler and Samuel's model. The result shows that the decline of the outflow for reduced winds continues right down to zero wind stress, as extrapolated by TS93. For stronger winds the slope becomes smaller, consistent with TS93's 1.5 $\times$  experiment.

Our restoring boundary condition experiment thus reproduces the findings of Toggweiler and Samuels, while our experiment with the hybrid coupled model does not. A direct comparison of the (filtered) response of both is given in Fig. 10. This reveals that the sensitivity in the strong wind range is quite similar for both models, but that only the model with restoring conditions is sensitive to a reduction in wind stress below present-day values. The cause of this difference must be the thermal feedback discussed in the next section.

### c. Thermal feedback effect

The stabilizing role that thermal feedback plays for the thermohaline circulation is now well understood (Rahmstorf and Willebrand 1995). Reduced overturning and heat transport leads to surface cooling in the deep-water formation region, which enhances the density and counteracts the reduction in overturning. Rahmstorf (1995c) has shown in a series of idealized experiments, using the same simple atmosphere model as used here, that it is this feedback that largely regulates the thermohaline overturning rate. With a restoring boundary condition on temperature, this feedback is all but suppressed.

The operation of this feedback in our wind sensitivity experiments is demonstrated in Fig. 11. In the case of

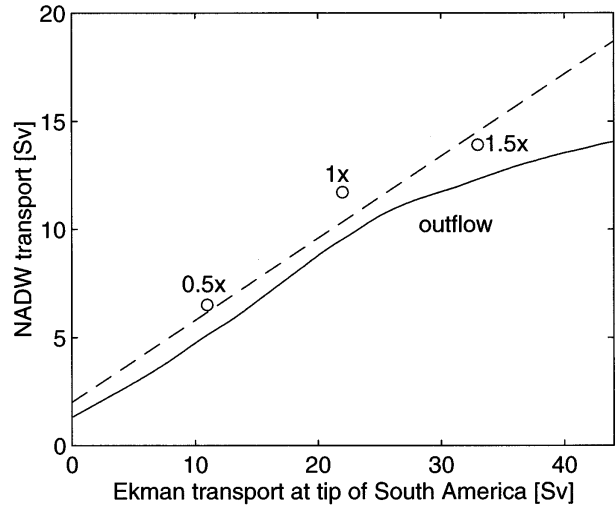


FIG. 9. Atlantic outflow for the model with restoring boundary conditions (solid line) as in Fig. 8 but with the oscillations removed. For comparison the results of the 0.5 $\times$ , 1 $\times$ , and 1.5 $\times$  runs of TS93 and the regression line of TS93 are shown.

the hybrid model, the mean high-latitude temperature in the North Atlantic varies by 2 $^{\circ}$ C for a 10-Sv overturning change; the heat loss averaged over the same high-latitude area varied by 16 W m $^{-2}$ . The 2-degree cooling corresponds (for fixed salinity) to a density increase of 0.29 kg m $^{-3}$ ; from the regression shown in Rahmstorf (1996b) we see that such a density change would drive an overturning increase of about 9 Sv. This number is of course only a rough estimate, but amply demonstrates the power of thermal feedback. In case of restoring boundary conditions (Fig. 11b), the slope is almost an order of magnitude smaller (0.03 $^{\circ}$ C/Sv), making this feedback ineffective in regulating the flow. In its lower left part, Fig. 11a also shows ellipses associated

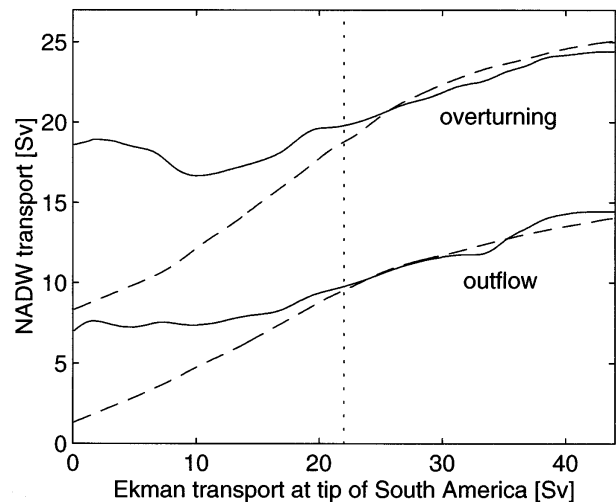


FIG. 10. Comparison of the Atlantic overturning and outflow (smoothed and with oscillations removed) for the hybrid model (solid) and the model with restoring boundary conditions (dashed).

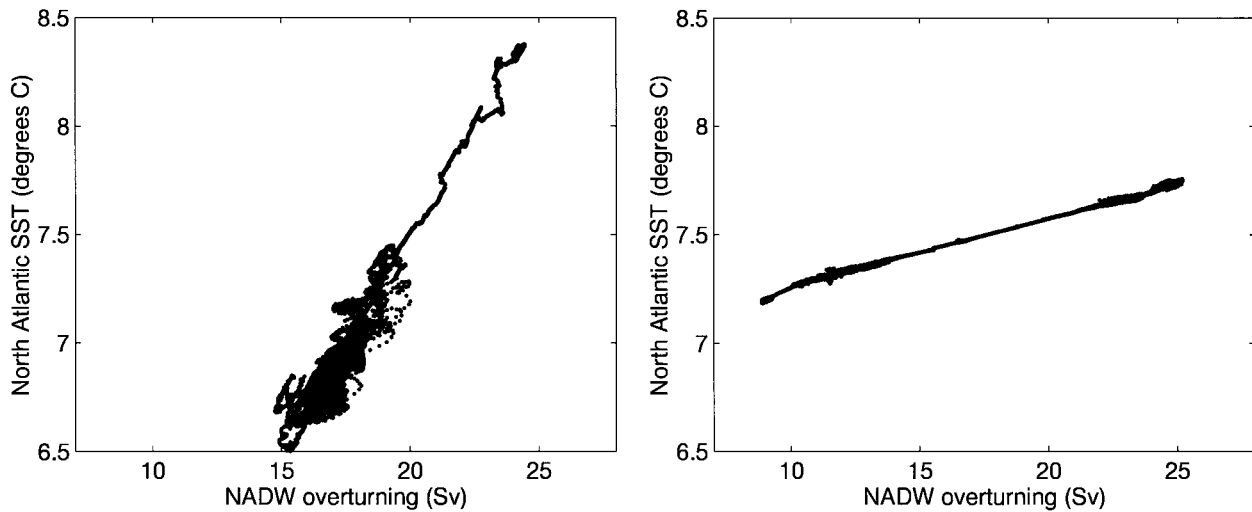


FIG. 11. North Atlantic SST averaged over the region north of 49°N and south of the Greenland–Scotland sill (~65°N), plotted as function of the Atlantic overturning (a) for the hybrid model with temperature feedback and (b) for the model with restoring boundary conditions. Each dot represents one annual value.

with the interdecadal oscillations. The major axis of these ellipses has a slope of 0.07°C/Sv, showing that on the decadal timescale the temperature response to overturning changes is only about a third of the equilibrium response.

The action of the temperature feedback explains why in Fig. 10 in the hybrid model the NADW flow does not decline much for a reduction in Southern Ocean wind stress, although it does with restoring boundary conditions. If the “conveyor belt” flow in the Atlantic gets weaker, the northern Atlantic temperatures cool sufficiently to maintain the thermal driving of the flow. This cannot happen if the temperatures are prevented from adjusting and continue to be restored to warmer conditions that correspond to a stronger overturning. In the hybrid model the NADW outflow reaches a thermally driven minimum level of about 7 Sv irrespective

of the winds in the Southern Ocean; only when the wind is almost as strong as in present conditions does it start to enhance the overturning and outflow in the North Atlantic somewhat. One could thus interpret the outflow for present-day conditions in the hybrid model as ~7 Sv thermally driven flow and 2–3 Sv attributable to the action of Southern Ocean winds. Note that this wind effect here includes the indirect effect that the wind forcing has on thermohaline flow by changing the temperature and salinity fields.

The pattern of surface temperature change is an interesting result of the present study and is shown in Fig. 12. The northern North Atlantic is seen to cool between 0.5° and 1°C in response to a 40% reduction in Southern Ocean wind stress, due to reduced heat transport in the Atlantic conveyor belt. Temperatures in the Southern Ocean change even more as the Antarctic Circumpolar Current (ACC) is weakened: the Atlantic sector gets colder, while the Pacific sector warms. The ACC transports heat from the Pacific to the Atlantic in our model; the changes shown in Fig. 12 are a consequence of the reduction in this heat transport.

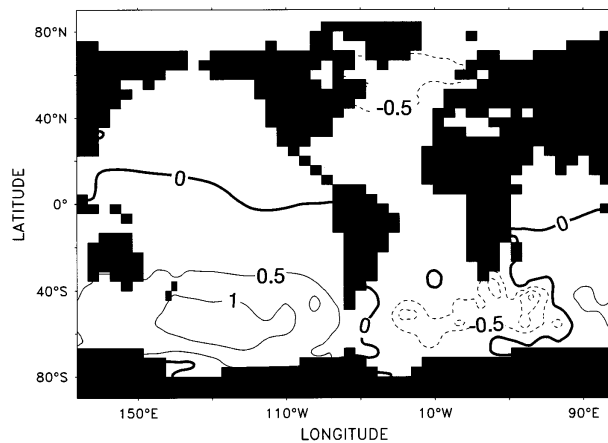


FIG. 12. Sea surface temperature difference between the experiment with 0.6 times the present wind stress in the Southern Ocean and the spinup state of the model, contour interval 0.5°C.

*d. Spatial structure of the circulation changes*

Thus far we have only looked at some key circulation indicators, but not at the spatial structure of the wind-induced circulation changes. Figures 13–15 show the meridional mass transport streamfunctions for the initial state and after a Southern Ocean wind stress decrease and increase by 40%. The present-day state (Fig. 13) has the familiar circulation cells in the Atlantic with a North Atlantic overturning of 20 Sv, a NADW outflow across 30°S of 10 Sv, and an AABW cell of 7 Sv. The Pacific has the desired two-cell structure with deep northward inflow, southward flow between 1.5 and 3

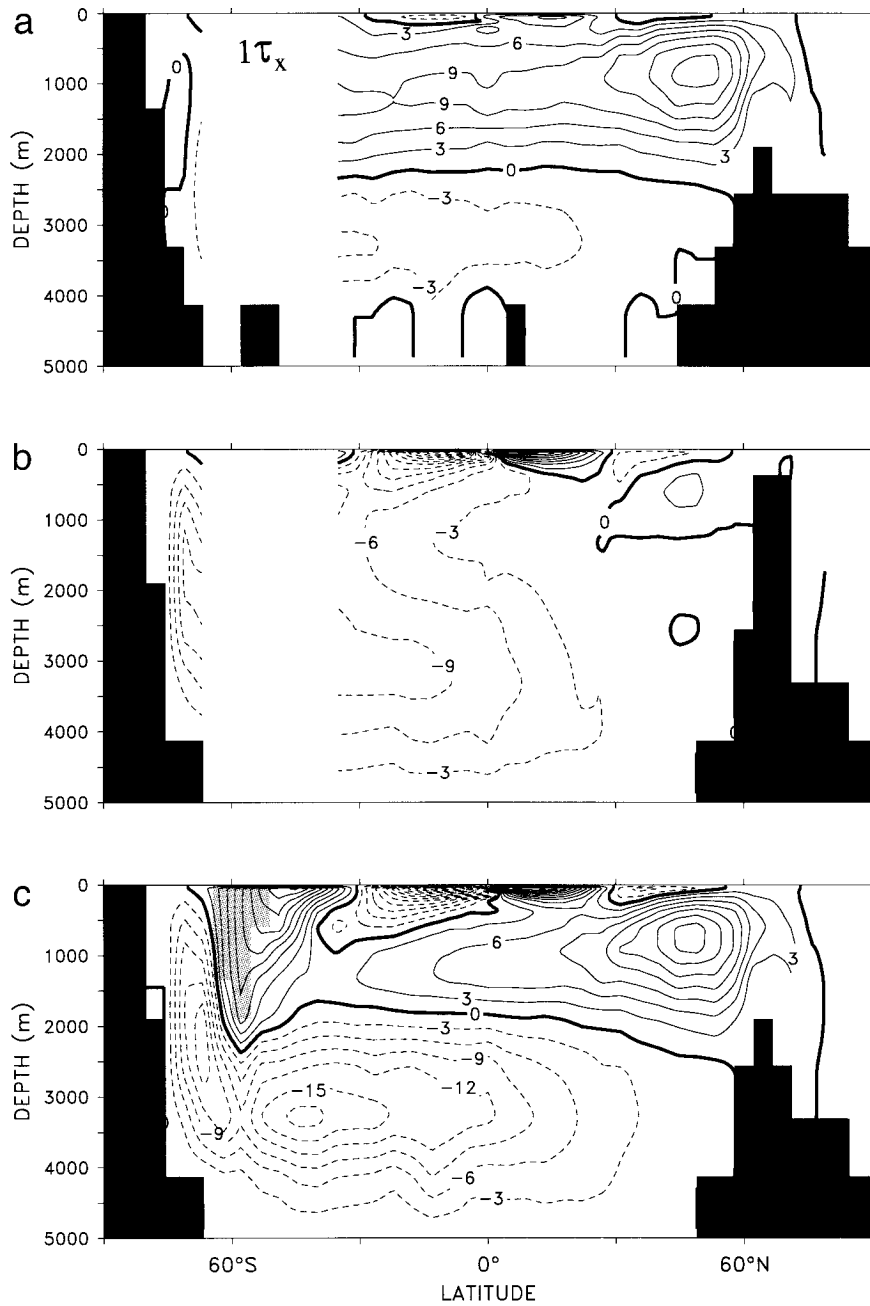


FIG. 13. Meridional transport streamfunctions for (a) the Atlantic Ocean, (b) the Indian/Pacific Ocean, and (c) the global ocean at the end of the spinup of the hybrid model.

km depth and northward flow of intermediate and surface waters (Toggweiler and Samuels 1993b).

The global streamfunction shows the Deacon cell near 60°S; this reaches less deep than in TS93 because of our shallower topography, but clearly reflects the obstacle that the Drake Passage gap (shaded in the figure) presents for meridional flow. The three other Ekman cells farther north are closed within the upper kilometer at most, but in the Deacon cell most of the return flow occurs below the sill depth. South of the Deacon cell

is the Antarctic cell, with a flow of 16 Sv in the hybrid model and 25 Sv in our model with restoring conditions. The sinking branch of this cell is not fed by surface flows, as in the Deacon cell, but by a poleward flow extending down to over 2000-m depth. The sinking is located at a deep convection site at the eastern end of the Ross Sea, which is the only place so far south that is deeper than 3300 m. Here 12 Sv downwell across the 2000-m depth level at only two grid points, in the region between 71.1° and 75.6°S, 153.8° and 142.5°W. It is not

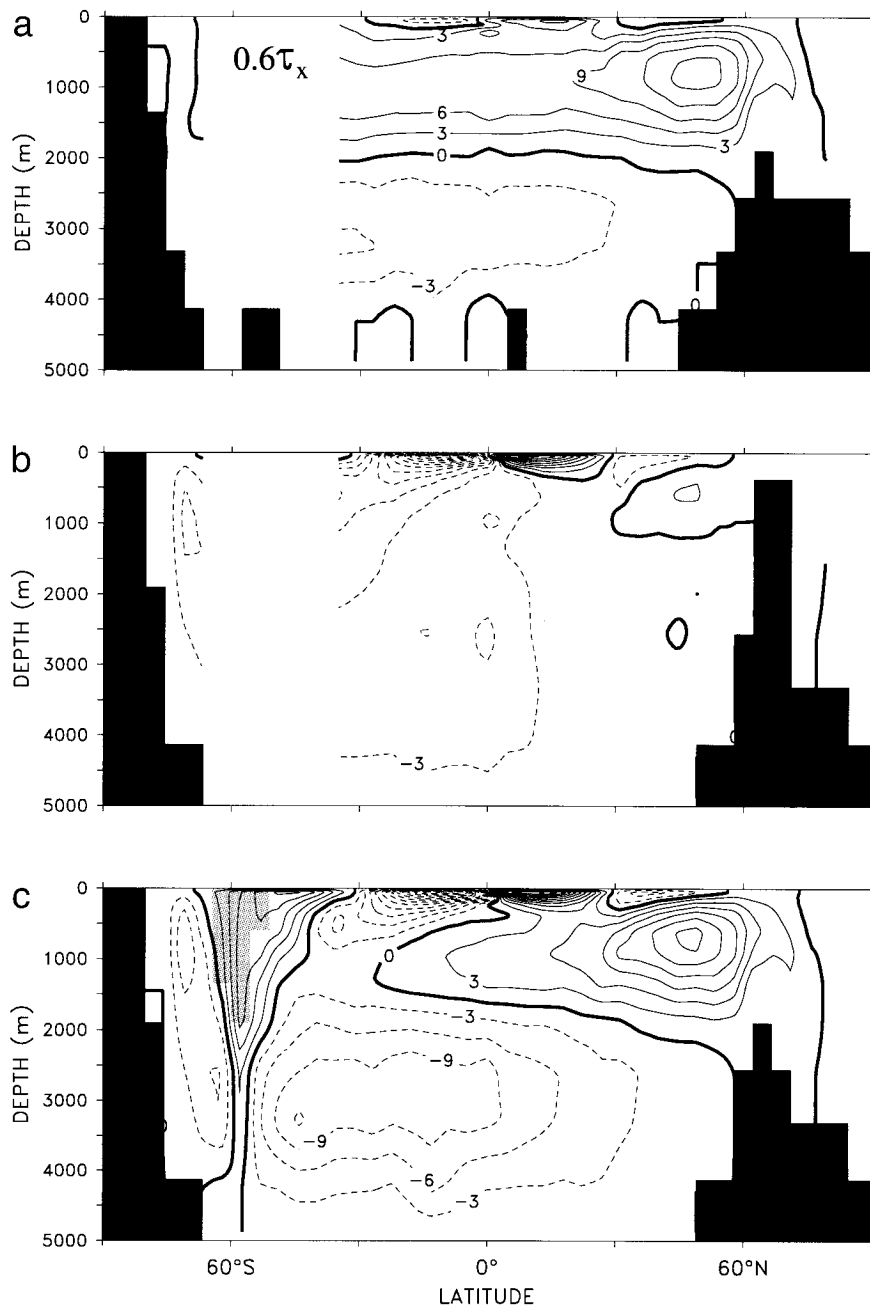


FIG. 14. As in Fig. 13 but after the zonal wind stress in the Southern Ocean had decreased to 0.6 times its present value.

clear why this Antarctic cell, which represents the formation of bottom water near Antarctica, is absent in the TS93 model. Our salinity correction off Tierra del Fuego (see section 2a) is not the reason, as we also obtain this cell without it. Therefore, the differences in topography appear the most likely cause. These differences in the Antarctic and Deacon cells do not seem to affect the sensitivity of the Atlantic outflow to Southern Ocean wind changes, however, as this is essentially the same

in our experiment with restoring boundary conditions and in the TS93 experiments.

In case of decreased or increased wind stress the Atlantic overturning (Figs. 14a and 15a) maintains its characteristic pattern, with only some adjustment in amplitude. When the wind stress is reduced even further toward zero, the NADW overturning cell does not change significantly but the AABW flow becomes unstable, as discussed earlier.

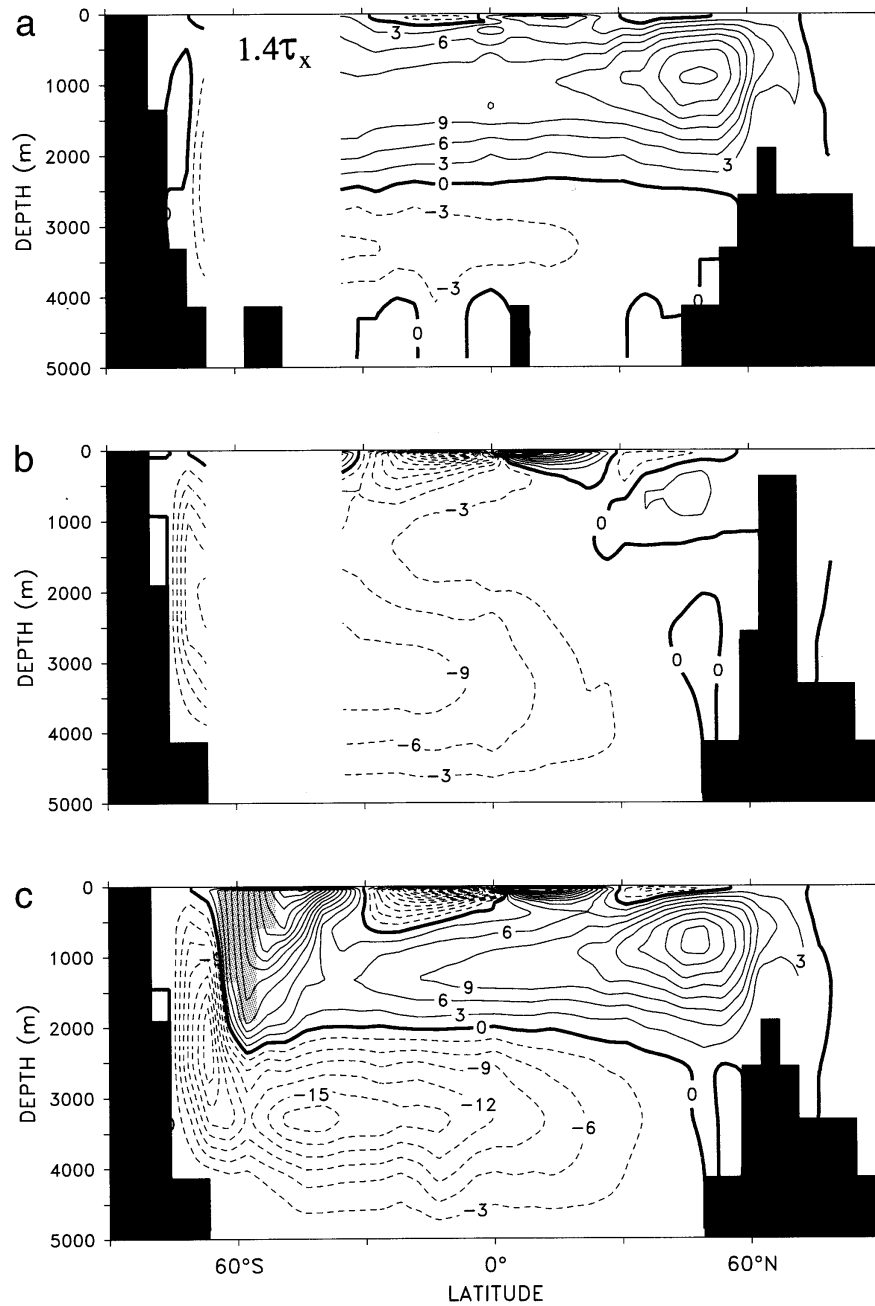


FIG. 15. Same as Fig. 13 but after the zonal wind stress in the Southern Ocean had risen to 1.4 times its present value.

The flow in the Pacific is largely insensitive to a wind increase in the Southern Ocean (Fig. 15b), but when the wind is decreased (Fig. 14b) the two-cell structure is lost. The strong bottom water inflow of 10 Sv below 3000 m and its southward return flow between 1500- and 3000-m depth have disappeared and, instead, there is a sluggish northward flow across the whole depth range.

In the global picture (Figs. 13c–15c) we see that not only the strength of the Deacon cell but also that of the

Antarctic cell is roughly proportional to the zonal wind stress over the Southern Ocean. The overturning in the Antarctic cell and the strength of the ACC may be connected through the interaction of density gradients with topography. For vanishing wind stress (not shown) both cells disappear (including the downwelling branch of the Deacon cell, in contrast to the assertion of TS95 that this downwelling is buoyancy forced). The bottom water cell also all but disappears in the absence of wind, and is substantially reduced in the  $0.6\tau_x$  case. However,

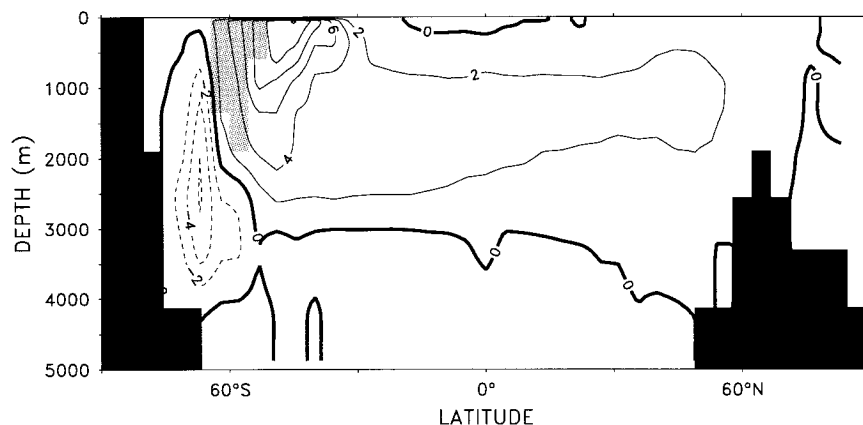


FIG. 16. Difference in global overturning between Figs. 15 and 13. The overturning change shown here is the result of a 40% increase in Southern Ocean zonal wind stress.

an increase in wind stress beyond present levels has no effect on this cell; it seems to have reached a saturation level beyond which it cannot be forced by Southern Ocean winds. The apparent wind dependence of the bottom waters of Antarctic origin deserves further study.

The North Atlantic cell and the Deacon cell appear disconnected in Fig. 14c as if the proposed link between the two were broken. But this merely highlights the dangers of interpreting zonally integrated flow diagrams, as Figs. 14a and 14b show (see also the discussion in the next section). What appears like a reduced southward extension of the Atlantic cell is, in fact, largely due to changes in the Pacific.

Another aspect of the Deacon cell, which is not visible in the overturning streamfunction, is that the upwelling in this cell completely changes its character with depth. Near the surface there is a widespread band of upwelling circling the globe between  $45^{\circ}$  and  $70^{\circ}$ S, due to the Ekman divergence. Farther down in the water column, however, upwelling is almost exclusively confined to the southern half of Drake Passage. At four model grid cells spanning the region  $57.8^{\circ}$ – $66.7^{\circ}$ S,  $71.3^{\circ}$ – $63.8^{\circ}$ W 40 Sv upwell across the 2000-m depth level, partly counteracted by some downwelling along the Indian Ocean sector at the same latitude.

The *change* in overturning that arises from a 40% wind stress increase is shown in Fig. 16. The Deacon cell increases by 12 Sv at its maximum at  $44.5^{\circ}$ S. The Ekman drift increases by 8.6 Sv at  $53.3^{\circ}$ S (where geostrophic return flow is only possible below 600 m in our model) and by 5.6 Sv at  $57.8^{\circ}$ S (where geostrophic return flow is possible below 1900 m). Of the return flow in the Deacon cell, 9 Sv occur below 900-m depth, but only 3 Sv take the route via the North Atlantic.

Further understanding can be gained by looking at how the upwelling and downwelling (and their changes) are spread over the different ocean basins (Figs. 17 and 18). A vertical change in upwelling must, of course, be balanced by a divergence of horizontal flow at that level. Figure 17a shows an upwelling of 22 Sv to the surface

level in the Southern Ocean south of  $53.3^{\circ}$ S (solid line), which exactly balances the northward Ekman drift; 19 Sv of this comes from below the sill depth of 600 m, so the viscous “leakage” across the Drake Passage gap (discussed by TS95) is only 3 Sv. At  $57.8^{\circ}$ S (Fig. 18a) the picture is similar: of the upwelling 14 Sv that balances the Ekman drift across this latitude, over 11 Sv are drawn from below the sill at 1900 m. Similar results are also found for the upwelling *changes* shown in Figs. 17b and 18b. Ageostrophic flow made possible by the artificially high viscosity of the coarse model thus accounts for only a small part of the return flow.

In Figs. 17a and 18a the downwelling from the surface level north of  $53.3^{\circ}$  and  $57.8^{\circ}$ S respectively occurs in the different ocean basins almost exactly according to the proportion of Ekman drift in the corresponding longitude sectors. Net interbasin exchange in the top 50 m is understandably small compared to the Ekman drift since the ocean sections across which this interbasin flow can take place are small. However, the Ekman drift is confined to the top 50 m while the interbasin exchange is not, so that the latter gains in importance as we go deeper. Between 500 and 2000 m the Atlantic (dashed line) dominates the downwelling due to the formation of NADW; the 17 Sv that upwell south of  $53.3^{\circ}$ S across 900-m depth are almost exclusively balanced by downwelling in the Atlantic (Fig. 17a). Thus far, this is consistent with Toggweiler and Samuel’s theory. But if we look at the wind-induced *changes* in upwelling, we see that of the extra 9 Sv drawn up across 900 m by the wind increase in Fig. 17b, 6 Sv sink in the Atlantic, 4 Sv sink in the Pacific, while the Indian Ocean upwells an additional 1 Sv. Of the 6 Sv sinking in the Atlantic, only 3 Sv do so in the North Atlantic.

#### 4. Discussion and conclusions

The experiments reported here confirm Toggweiler and Samuel’s tantalizing idea of a teleconnection between the winds in the Southern Ocean and the circu-

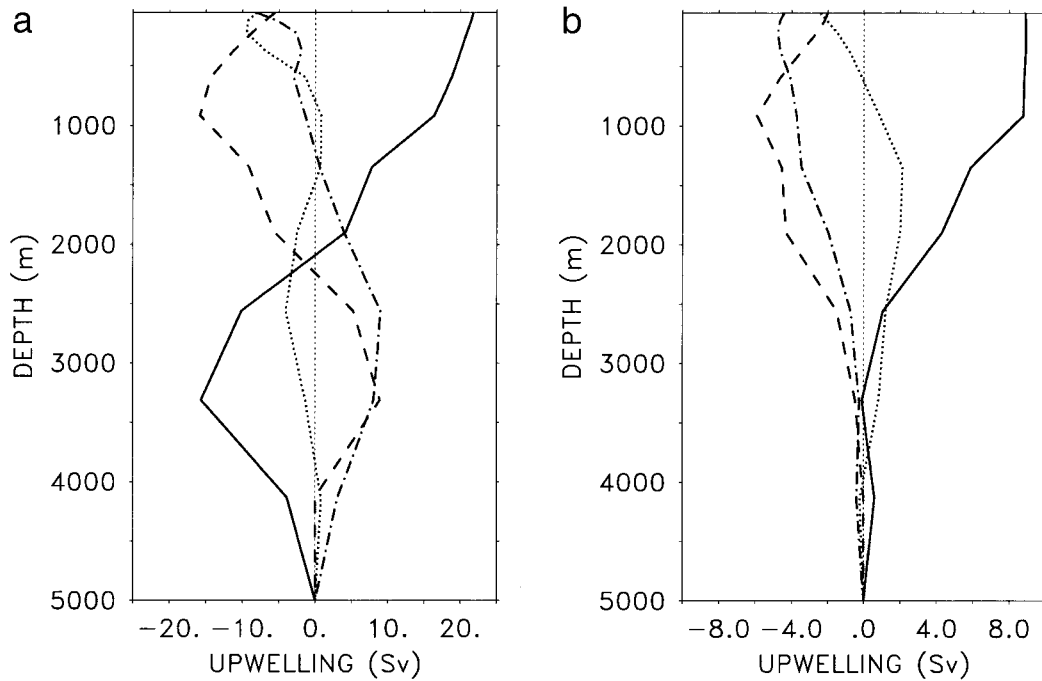


FIG. 17. Upwelling as function of depth, integrated over the Southern Ocean south of 53.3°S (solid), and north of this latitude over the Atlantic (dashed), the Indian Ocean (dotted), and the Pacific (dash-dotted): (a) for the spinup state of the model and (b) the *difference* arising from a 40% increase in Southern Ocean wind stress.

lation and climate of the North Atlantic. However, we found this teleconnection to be much weaker than originally suggested. Instead of the NADW outflow being *controlled* by Southern Hemisphere winds, we found it

to be somewhat *modulated* by these winds; the effect of thermohaline forcing clearly dominated the “Drake Passage effect” in our experiments. The dominance of the wind forcing in the Toggweiler and Samuels ex-

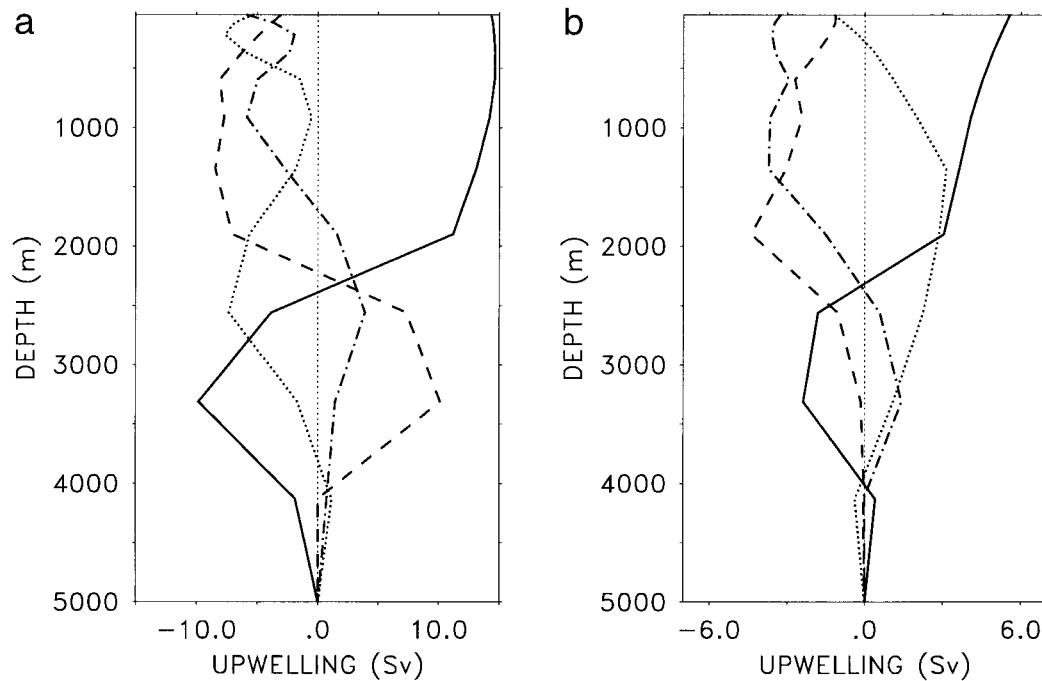


FIG. 18. As in Fig. 17 but with the integration limit at 57.8°S.

periments appears to be due to the use of a thermal restoring boundary condition and thus the neglect of temperature feedback, which was identified by Rahmstorf (1995c) as the major feedback regulating the overturning strength in the Atlantic. This negative feedback leads to cooler temperatures in high latitudes of the North Atlantic when the thermohaline overturning slows down, thus enhancing high-latitude density and counteracting the reduction in overturning.

In the light of these results, some of the arguments in favor of a controlling role of Southern Ocean winds for NADW outflow need to be reexamined. TS95 argue that the water pushed north in the Ekman drift can only “link up” with the southward flow at depth by passing through the North Atlantic, since sinking anywhere else is prohibited by strong density stratification. While this is a suggestive proposition when looking at meridional mass transport streamfunction plots (e.g., Fig. 13), it is not necessarily true in a three-dimensional flow. No individual water particle needs to follow the zonally integrated two-dimensional streamlines, and a zonal-mean net sinking can close the mass budget in the presence of density stratification without any water needing to make a large vertical excursion or needing to penetrate this stratification (Döös 1994). Indeed, most of the Ekman drift in our model recirculates locally (Fig. 16). Of the 9-Sv additional northward Ekman transport across 53.3°S that arise from a 40% wind stress increase, only 3 Sv sink in the North Atlantic as NADW, whereas the majority of 6 Sv downwells in the Southern Hemisphere. Only a negligible amount “leaks” back south above the topography due to the artificially high viscosity of the coarse model (Fig. 17b).

This raises the question whether the net sinking just north of Drake Passage may be a model artifact. We believe not, since the same phenomenon is found in the 2° resolution global model of Hirst et al. (1996) and in the eddy-resolving FRAM model (Döös 1994). Both papers analyze the Deacon cell in detail and find that its sinking branch consists largely of isopycnal flow and is thus consistent with the presence of density stratification—in an isopycnal or neutral surface representation, the Deacon cell all but disappears. Our experiments further show that the sinking between 30° and 50°S is not buoyancy forced since it disappears completely when the zonal wind stress over the Southern Ocean is reduced to zero.

TS95 and Toggweiler (1994) further argue that the intensity of diapycnal mixing observed in the ocean is too weak to drive the observed magnitude of deep circulation. The classic concept of a thermally driven deep circulation depends on the downward diffusion of heat as the ultimate driving force of the overturning (Sandström’s theorem; Sandström 1908), and simple scaling arguments require a diapycnal thermal diffusivity of the order of  $1 \text{ cm}^2 \text{ s}^{-1}$  to drive a deep circulation of the order of 10 Sv (e.g., see Rahmstorf 1995c). This seems at odds with microstructure measurements (Gregg 1987)

and tracer spreading experiments (Ledwell et al. 1993), which yield a diffusivity of only  $\sim 0.1 \text{ cm}^2 \text{ s}^{-1}$ . However, these values apply to the thermocline, which is not in simple upwelling–diffusion balance but ventilated by wind-driven flow (Luyten et al. 1983). Of more direct relevance for the deep circulation are mixing rates in the deep ocean. Recently, Kunze and Sanford (1996) showed that deep mixing over flat abyssal plains is likewise only  $\sim 0.1 \text{ cm}^2 \text{ s}^{-1}$ . On the other hand, mixing over rough terrain and near boundaries can be much larger than  $1 \text{ cm}^2 \text{ s}^{-1}$  throughout the water column (Polzin et al. 1997). Marotzke (1997) has demonstrated in numerical model experiments that a boundary mixing of, for example,  $5 \text{ cm}^2 \text{ s}^{-1}$  with no interior vertical mixing can drive a meridional overturning of 18 Sv. Boundary mixing turned out to be more effective in driving deep flow than uniform mixing with the same basin-average value. It is thus not clear whether there really is a “missing mixing problem” as discussed in Toggweiler (1994) or whether ocean mixing is, in fact, large enough to drive the observed deep circulation.

Another argument put forward for the Drake Passage effect is that there apparently is a threshold value for the NADW outflow; this is interpreted by TS93 as indicating that, once NADW outflow is established, its magnitude is dictated by the Southern Ocean wind or that at least the Ekman drift sets a lower limit by “locking on” to the NADW outflow (TS95). A physical mechanism for this locking on and how it leads to a threshold was not described. However, there is a well-understood mechanism for the existence of such a threshold if the outflow is thermohaline-driven rather than controlled by the wind. This mechanism is the positive salt transport feedback, which was demonstrated for a one-hemisphere box model in Stommel’s (1961) classic paper and extended and applied to the cross-hemispheric NADW flow in Rahmstorf (1996b). The latter shows that the response of a global model (the same as used in this study) to changes in freshwater forcing clearly shows Stommel’s bifurcation and is in excellent agreement with the purely thermohaline theory of the deep circulation, which could not be the case if the NADW flow was controlled by the wind.

In conclusion, we find no compelling theoretical reasons for a control of NADW outflow by Southern Hemisphere winds, and in our experiments the influence of these winds is only moderate. The model results do not resolve the question of whether the wind influence works directly in the way the near-surface Ekman cells are forced or indirectly through altering the heat or freshwater budget (and thus density) of the South Atlantic, as was speculated by Hughes (1995). For example, Rahmstorf (1996b) predicts a strong sensitivity of the NADW circulation to the wind-driven freshwater transport into the South Atlantic, which could provide a possible link between Southern Hemisphere winds and NADW flow.

The general sensitivity of the Atlantic deep circula-

tion to changes in thermohaline forcing has been amply demonstrated in recent years (see reviews by Rahmstorf et al. 1996; Weaver and Hughes 1992) and appears to be much stronger than the sensitivity to wind forcing. Our results thus support the classic view of the Atlantic deep circulation being predominantly thermohaline-driven rather than driven by the winds over the Southern Ocean. They further indicate, however, that the formation of bottom water near Antarctica may depend strongly on those winds.

*Acknowledgments.* The authors greatly benefited from numerous stimulating discussions with H. Van den Budenmeyer. This research was funded by the European Union's Environment and Climate Programme and by the Australian Research Council.

## REFERENCES

- Bryan, K., 1984: Accelerating the convergence to equilibrium of ocean-climate models. *J. Phys. Oceanogr.*, **14**, 666–673.
- Cox, M. D., 1989: An idealized model of the world ocean. Part I: The global scale water masses. *J. Phys. Oceanogr.*, **19**, 1730–1752.
- Döös, K., 1994: The Deacon cell and the other meridional cells of the Southern Ocean. *J. Phys. Oceanogr.*, **24**, 429–442.
- England, M. H., 1992: The global-scale circulation and water-mass formation in a world ocean model. Ph.D. thesis, Dept. of Geology and Geophysics, University of Sydney, 226 pp. [Available from Department of Geology and Geophysics, Edgeworth David Building, F05, The University of Sydney, Sydney, NSW 2006, Australia.]
- Gregg, M. C., 1987: Diapycnal mixing in the thermocline: A review. *J. Geophys. Res.*, **92**, 5249–5286.
- Hellerman, S., and M. Rosenstein, 1983: Normal monthly wind stress over the world ocean with error estimates. *J. Phys. Oceanogr.*, **13**, 1093–1104.
- Hirst, A. C., D. Jackett, and T. McDougall, 1996: The meridional overturning cells of a World Ocean model in neutral surface coordinates. *J. Phys. Oceanogr.*, **26**, 775–791.
- Hughes, T. M. C., 1995: Uniqueness and variability of the ocean's thermohaline circulation. Ph.D. thesis, Dept. of Atmospheric and Oceanic Sciences, McGill University, 216 pp. [Available from Dept. of Atmospheric and Oceanic Sciences, McGill University, Montreal, QC H3A 2K6 Canada.]
- , and A. J. Weaver, 1994: Multiple equilibria of an asymmetric two-basin ocean model. *J. Phys. Oceanogr.*, **24**, 619–637.
- , and —, 1996: Sea surface temperature–evaporation feedback and the ocean's thermohaline circulation. *J. Phys. Oceanogr.*, **26**, 644–654.
- Kawase, M., 1987: Establishment of deep circulation driven by deep water production. *J. Phys. Oceanogr.*, **17**, 2294–2316.
- Kunze, E., and T. B. Sanford, 1996: Abyssal mixing: Where it is not. *J. Phys. Oceanogr.*, **26**, 2286–2296.
- Ledwell, J. R., A. J. Watson, and C. S. Law, 1993: Evidence for slow mixing across the pycnocline from an open-ocean tracer release experiment. *Nature*, **364**, 701–703.
- Levitus, S., 1982: *Climatological Atlas of the World Ocean*. NOAA Prof. Paper No. 13, U.S. Govt. Printing Office, 173 pp.
- Luyten, J. R., J. Pedlosky, and H. Stommel, 1983: The ventilated thermocline. *J. Phys. Oceanogr.*, **13**, 292–309.
- Manabe, S., and R. J. Stouffer, 1988: Two stable equilibria of a coupled ocean–atmosphere model. *J. Climate*, **1**, 841–866.
- Marotzke, J., 1997: Boundary mixing and the dynamics of three-dimensional thermohaline circulations. *J. Phys. Oceanogr.*, **27**, 1713–1728.
- McDermott, D. A., 1996: The regulation of northern overturning by Southern Hemisphere winds. *J. Phys. Oceanogr.*, **26**, 1234–1255.
- Mikolajewicz, U., and E. Maier-Reimer, 1994: Mixed boundary conditions in OGCMs and their influence on the stability of the model's conveyor belt. *J. Geophys. Res.*, **99**, 22 633–22 644.
- Pacanowski, R., K. Dixon, and A. Rosati, 1991: The GFDL modular ocean model users guide. Vol. 2, GFDL, Princeton, 376 pp. [Available from GFDL, Box 308, Princeton, NJ 08540.]
- Polzin, K., J. M. Toole, J. R. Ledwell, and R. W. Schmitt, 1997: Spatial variability of turbulent mixing in the abyssal ocean. *Science*, **276**, 93–96.
- Rahmstorf, S., 1993: A fast and complete convection scheme for ocean models. *Ocean Modelling*, **101**, (unpublished manuscripts), 9–11.
- , 1995a: Bifurcations of the Atlantic thermohaline circulation in response to changes in the hydrological cycle. *Nature*, **378**, 145–149.
- , 1995b: Climate drift in an OGCM coupled to a simple, perfectly matched atmosphere. *Climate Dyn.*, **11**, 447–458.
- , 1995c: Multiple convection patterns and thermohaline flow in an idealized OGCM. *J. Climate*, **8**, 3028–3039.
- , 1996a: Comment on “Instability of the thermohaline circulation with respect to mixed boundary conditions.” *J. Phys. Oceanogr.*, **26**, 1099–1105.
- , 1996b: On the freshwater forcing and transport of the Atlantic thermohaline circulation. *Climate Dyn.*, **12**, 799–811.
- , and J. Willebrand, 1995: The role of temperature feedback in stabilizing the thermohaline circulation. *J. Phys. Oceanogr.*, **25**, 787–805.
- , J. Marotzke, and J. Willebrand, 1996: Stability of the thermohaline circulation. *The Warm Water Sphere of the North Atlantic Ocean*, W. Krauss, Ed., Borntraeger, 129–158.
- Sandström, J. W., 1908: Dynamische Versuche mit Meerwasser. *Ann. Hydrogr. Man. Meteor.*, **36**, 6–23.
- Semtner, A. J., and R. M. Chervin, 1992: Ocean general circulation from a global eddy-resolving model. *J. Geophys. Res.*, **97**(C4), 5493–5550.
- Stommel, H., 1961: Thermohaline convection with two stable regimes of flow. *Tellus*, **13**, 224–230.
- Toggweiler, J. R., 1994: The ocean's overturning circulation. *Phys. Today*, **47**(11), 45–50.
- , and B. Samuels, 1993a: Is the magnitude of the deep outflow from the Atlantic Ocean actually governed by Southern Hemisphere winds? *The Global Carbon Cycle*, M. Heimann, Ed., Springer, 303–331.
- , and —, 1993b: New radiocarbon constraints on the upwelling of abyssal water to the ocean's surface. *The Global Carbon Cycle*, M. Heimann, Ed., Springer, 333–366.
- , and —, 1995: Effect of Drake Passage on the global thermohaline circulation. *Deep-Sea Res.*, **42**, 477–500.
- Weaver, A. J., and T. M. C. Hughes, 1992: Stability and variability of the thermohaline circulation and its link to climate. *Trends in Physical Oceanography*, Council of Scientific Research Integration, 15–70.